

## Holographic Thermalization, Stability of Anti-de Sitter Space, and the Fermi-Pasta-Ulam Paradox

Venkat Balasubramanian,<sup>1,\*</sup> Alex Buchel,<sup>1,2,†</sup> Stephen R. Green,<sup>3,‡</sup> Luis Lehner,<sup>2,§</sup> and Steven L. Liebling<sup>4,||</sup>

<sup>1</sup>*Department of Applied Mathematics, University of Western Ontario, London, Ontario N6A 5B7, Canada*

<sup>2</sup>*Perimeter Institute for Theoretical Physics, Waterloo, Ontario N2L 2Y5, Canada*

<sup>3</sup>*Department of Physics, University of Guelph, Guelph, Ontario N1G 2W1, Canada*

<sup>4</sup>*Department of Physics, Long Island University, Brookville, New York 11548, USA*

(Received 1 April 2014; revised manuscript received 25 May 2014; published 13 August 2014)

For a real massless scalar field in general relativity with a negative cosmological constant, we uncover a large class of spherically symmetric initial conditions that are close to anti-de Sitter space (AdS) but whose numerical evolution does not result in black hole formation. According to the AdS/conformal field theory (CFT) dictionary, these bulk solutions are dual to states of a strongly interacting boundary CFT that fail to thermalize at late times. Furthermore, as these states are not stationary, they define dynamical CFT configurations that do not equilibrate. We develop a two-time-scale perturbative formalism that captures both direct and inverse cascades of energy and agrees with our fully nonlinear evolutions in the appropriate regime. We also show that this formalism admits a large class of quasiperiodic solutions. Finally, we demonstrate a striking parallel between the dynamics of AdS and the classic Fermi-Pasta-Ulam-Tsingou problem.

DOI: 10.1103/PhysRevLett.113.071601

PACS numbers: 11.25.Tq, 04.20.-q, 05.45.-a, 11.10.-z

*Introduction.*—The gauge theory–string theory correspondence [1] has become a valuable tool to study non-equilibrium phenomena in strongly interacting quantum field theories [2–4]. In a particular limit, this correspondence links general relativity (GR) in  $(d + 1)$ -dimensional asymptotically anti-de Sitter (AdS<sub>*d*+1</sub>) spacetimes with *d*-dimensional conformal field theories. A question of particular importance in field theory is to understand the process of equilibration and thermalization. This corresponds, in the bulk, to the collapse of an initial perturbation to a black hole.

In the first detailed analysis [5] of the dynamics of perturbations of global AdS<sub>4</sub>, Bizoń and Rostworowski argued that (except for special *nonresonant* initial data) the evolution of a real, massless, spherically symmetric scalar field *always* results in gravitational collapse, even for arbitrarily small initial field amplitude  $\epsilon$ . At the linear level, this system is characterized by a normal mode spectrum with natural frequencies  $\omega_j = 2j + 3$ . Using weakly nonlinear perturbation theory, these authors described the onset of instability as a result of resonant interactions between the normal modes. Because of the presence of a vast number of resonances, they argued that this mechanism leads to a *direct turbulent cascade* of energy to high mode numbers, making gravitational collapse inevitable. Higher mode numbers are more sharply peaked, so this corresponds to an effect of gravitational focusing.

The analysis of Ref. [5] also showed that, for initial data consisting of a single mode, the dominant effect of resonant self-interaction could be absorbed into a constant shift in the frequency of the mode. (This time-periodic solution was confirmed to persist at higher nonlinear order [6].)

However, for two-mode initial data, additional resonances are present that cannot be absorbed into frequency shifts. The result is secular growth of higher modes.

The turbulent cascade described in Ref. [5] is a beautiful mechanism for the thermalization of strongly coupled quantum field theories with holographic gravitational duals. However, it was recently pointed out that this cascade argument breaks down if *all* modes are initially populated, and the mode amplitudes fall off sufficiently rapidly for high mode numbers [7]. In this case, all resonant effects may once again be absorbed into frequency shifts and black hole collapse is avoided. Low-lying modes have broadly distributed bulk profiles. Thus, one might expect that if the initial scalar profile is broadly distributed, its evolution might not result in gravitational collapse (see also Refs. [8–10]). This prediction was verified numerically [11]. The physical mechanism responsible for the collapse or noncollapse of small amplitude initial data is a competition between two effects: gravitational focusing and nonlinear dispersion of the propagating scalar field. If the former dominates, gravitational collapse ensues [5]. If the latter does, the system evolves without approaching any identifiable static or stationary solution—the perturbed boundary CFT neither thermalizes nor equilibrates at late times [11].

The perturbation theory of Ref. [5] cannot make predictions at late times. (The growth of secular terms in the expansion causes a breakdown at time  $t \propto 1/\epsilon^2$ .) It also does not properly take into account energy transfer between modes. In this Letter, we undertake a thorough analysis of the dynamics of AdS by making use of a new perturbative formalism for analyzing the effect of resonances on the

evolution of this system *that is valid for long times*. We also perform fully nonlinear GR simulations (see Refs. [7,11] for details of our numerical implementation and validation). In the process, we uncover a close relationship between the dynamics of AdS and the famous Fermi-Pasta-Ulam-Tsingou (FPUT) problem [12,13]. Our formalism is based on a two-time-scale approach [14], where we introduce a new “slow time”  $\tau = \epsilon^2 t$ . The time scale  $\tau$  characterizes energy transfers between modes, whereas the “fast time”  $t$  characterizes the original normal modes. Importantly, this formalism allows one to study the system for long times and examine energy transfer between modes. In the following, we describe the “two time framework” (TTF) and determine a large class of quasiperiodic solutions that extends the single-mode periodic solutions of Refs. [5,6]. These solutions have finely tuned energy spectra such that the net energy flow into each mode vanishes, and they appear to be stable to small perturbations within both TTF and full numerical simulations. We then study the behavior of two-mode initial data of Ref. [5] under both approaches. Finally, we use the TTF equations to draw an interesting parallel between scalar collapse in AdS and the FPUT problem of thermalization of nonlinearly coupled oscillators [12].

*Model.*—Following Ref. [5], we consider a self-gravitating, real scalar field  $\phi$  in asymptotically AdS<sub>4</sub> spacetime. Imposing spherical symmetry, the metric takes the form

$$ds^2 = \frac{1}{\cos^2 x} (-Ae^{-2\delta} dt^2 + A^{-1} dx^2 + \sin^2 x d\Omega^2), \quad (1)$$

where we set the asymptotic AdS radius to 1. Spherical symmetry implies that  $A$ ,  $\delta$ , and  $\phi$  are functions of time  $t \in (-\infty, \infty)$  and the radial coordinate  $x \in [0, \pi/2)$ .

In terms of the variables  $\Pi \equiv e^\delta \dot{\phi}/A$  and  $\Phi \equiv \phi'$ , the equation of motion for  $\phi$  is

$$\ddot{\phi} = (\dot{A}e^{-\delta} - A\dot{\delta}e^{-\delta})\Pi + A^2 e^{-2\delta} \Phi' + \left( \frac{2}{\sin x \cos x} A^2 e^{-2\delta} + AA' e^{-2\delta} - A^2 e^{-2\delta} \delta' \right) \Phi, \quad (2)$$

while the Einstein equation reduces to the constraints,

$$A' = \frac{1 + 2\sin^2 x}{\sin x \cos x} (1 - A) + \sin x \cos x A (|\Phi|^2 + |\Pi|^2), \quad (3)$$

$$\delta' = -\sin x \cos x (|\Phi|^2 + |\Pi|^2). \quad (4)$$

*Two time framework.*—TTF consists of defining the slow time  $\tau = \epsilon^2 t$  and expanding the fields as

$$\phi = \epsilon \phi_{(1)}(t, \tau, x) + \epsilon^3 \phi_{(3)}(t, \tau, x) + O(\epsilon^5), \quad (5)$$

$$A = 1 + \epsilon^2 A_{(2)}(t, \tau, x) + O(\epsilon^4), \quad (6)$$

$$\delta = \epsilon^2 \delta_{(2)}(t, \tau, x) + O(\epsilon^4). \quad (7)$$

It is possible to go beyond  $O(\epsilon^3)$  by introducing additional slow time variables. However, the order of approximation used here is sufficient to capture the key aspects of weakly nonlinear AdS collapse in the  $\epsilon \rightarrow 0$  limit.

Perturbative equations are derived by substituting the expansions (5)–(7) into the equations of motion (2)–(4) and equating powers of  $\epsilon$ . It is important to note that when taking time derivatives of a function of both time variables we have  $\partial_t \rightarrow \partial_t + \epsilon^2 \partial_\tau$ . At  $O(\epsilon)$ , we obtain the wave equation for  $\phi_{(1)}$  linearized off exact AdS,

$$\partial_t^2 \phi_{(1)} = \phi_{(1)}'' + \frac{2}{\sin x \cos x} \phi_{(1)}' \equiv -L \phi_{(1)}. \quad (8)$$

The operator  $L$  has eigenvalues  $\omega_j^2 = (2j+3)^2$  ( $j = 0, 1, 2, \dots$ ) and eigenvectors  $e_j(x)$  (“oscillons”) [5]. Explicitly,

$$e_j(x) = d_j \cos^3 x {}_2F_1\left(-j, 3 + j; \frac{3}{2}; \sin^2 x\right), \quad (9)$$

with  $d_j = 4\sqrt{(j+1)(j+2)}/\sqrt{\pi}$ . The oscillons form an orthonormal basis under the inner product

$$(f, g) = \int_0^{\pi/2} f(x)g(x)\tan^2 x dx. \quad (10)$$

The general real solution to Eq. (8) is

$$\phi_{(1)}(t, \tau, x) = \sum_{j=0}^{\infty} (A_j(\tau) e^{-i\omega_j t} + \bar{A}_j(\tau) e^{i\omega_j t}) e_j(x), \quad (11)$$

where  $A_j(\tau)$  are arbitrary functions of  $\tau$ , to be determined later.

At  $O(\epsilon^2)$  the constraints (3)–(4) have solutions

$$A_{(2)}(x) = -\frac{\cos^3 x}{\sin x} \int_0^x (|\Phi_{(1)}(y)|^2 + |\Pi_{(1)}(y)|^2) \tan^2 y dy, \quad (12)$$

$$\delta_{(2)}(x) = -\int_0^x (|\Phi_{(1)}(y)|^2 + |\Pi_{(1)}(y)|^2) \sin y \cos y dy. \quad (13)$$

Finally, at  $O(\epsilon^3)$  we obtain the equation for  $\phi_{(3)}$ ,

$$\partial_t^2 \phi_{(3)} + L \phi_{(3)} + 2\partial_t \partial_\tau \phi_{(1)} = S_{(3)}(t, \tau, x), \quad (14)$$

where the source term is

$$S_{(3)} = \partial_t (A_{(2)} - \delta_{(2)}) \partial_t \phi_{(1)} - 2(A_{(2)} - \delta_{(2)}) L \phi_{(1)} + (A'_{(2)} - \delta'_{(2)}) \phi'_{(1)}. \quad (15)$$

The solutions (12)–(13) for  $A_{(2)}$  and  $\delta_{(2)}$  are substituted directly into  $S_{(3)}$ . In general, the source term  $S_{(3)}$  contains

resonant terms (i.e., terms proportional to  $e^{\pm i\omega_j t}$ ). As noted in Ref. [5], for all triads  $(j_1, j_2, j_3)$ , resonances occur at  $\omega_j = \omega_{j_1} + \omega_{j_2} - \omega_{j_3}$ . In ordinary perturbation theory, these resonances lead to secular growths in  $\phi_{(3)}$ . However, Ref. [5] showed that in *some* cases the growths may be absorbed into frequency shifts. TTF provides a natural way to handle these resonances by taking advantage of the new term  $2\partial_t \partial_\tau \phi_{(1)}$  in Eq. (14) and the freedom in  $A_j(\tau)$ .

We now project Eq. (14) onto an individual oscillon mode  $e_j$  and substitute for  $\phi_{(1)}$ ,

$$(e_j, \partial_\tau^2 \phi_{(3)} + \omega_j^2 \phi_{(3)}) - 2i\omega_j (\partial_\tau A_j e^{-i\omega_j t} - \partial_\tau \bar{A}_j e^{i\omega_j t}) = (e_j, S_{(3)}). \quad (16)$$

By exploiting the presence of terms proportional to  $e^{\pm i\omega_j t}$  on the left-hand side of the equation, we may cancel off the resonant terms on the right-hand side. Denoting by  $f[\omega_j]$  the part of  $f$  proportional to  $e^{i\omega_j t}$ , we set

$$-2i\omega_j \partial_\tau A_j = (e_j, S(t, \tau, x))[-\omega_j] = \sum_{klm} S_{klm}^{(j)} \bar{A}_k A_l A_m, \quad (17)$$

where  $S_{klm}^{(j)}$  are real constants representing different resonance channel contributions. The right-hand side is a cubic polynomial in  $A_j$  and  $\bar{A}_j$ . Thus, we have obtained a set of coupled first-order ordinary differential equations in  $\tau$  for  $A_j$ , which we shall refer to as the ‘‘TTF equations.’’ The equations are to be solved given the initial conditions for  $\phi$ . This procedure fixes the arbitrariness in the solution (11) for  $\phi_{(1)}$ . While we could also solve for  $\phi_{(3)}$ , this would be of little interest since the lack of resonances remaining in Eq. (14) implies that  $\phi_{(3)}$  remains bounded.

Under evolution via the TTF equations, both the amplitude and phase of the complex coefficients  $A_j(\tau)$  can vary. Thus, in contrast to the perturbative analysis in Ref. [5], the energy per mode  $E_j = \omega_j^2 |A_j|^2$  can change with time in a very nontrivial manner. However, it can be checked that the total energy  $E = \sum_j E_j$  is conserved. TTF, thus, describes an energy-conserving dynamical system. The TTF equations also possess a scaling symmetry  $A_j(\tau) \rightarrow \epsilon A_j(\tau/\epsilon^2)$ . This symmetry was observed in Fig. 2(b) of Ref. [5], which indicates that the instability mechanism is captured by TTF.

In practice, it is necessary to truncate the TTF equations at finite  $j = j_{\max}$ . We evaluated  $S_{klm}^{(j)}$  up to  $j_{\max} = 47$ . In particular, under truncation to  $j_{\max} = 0$ , the equations reduce to

$$i\pi \partial_\tau A_0 = 153 A_0^2 \bar{A}_0, \quad (18)$$

with solution  $A_0(\tau) = A_0(0) \exp(-i(153/\pi) |A_0(0)|^2 \tau)$ . This reproduces precisely the single-mode frequency shift result of Ref. [5].

*Quasiperiodic solutions.*—To understand the dynamics of TTF, we first look for quasiperiodic solutions. For

$j_{\max} = 0$ , this is the periodic solution above. For general  $j_{\max} > 0$  we take as ansatz  $A_j = \alpha_j \exp(-i\beta_j \tau)$ , where  $\alpha_j, \beta_j \in \mathbb{R}$  are independent of  $\tau$ . These solutions have  $E_j = \text{constant}$ , so they represent a balancing of energy fluxes such that each mode has constant energy. By substitution into the TTF equations, the  $\tau$  dependence can be canceled by requiring  $\beta_j = \beta_0 + j(\beta_1 - \beta_0)$ . This leaves  $j_{\max} + 1$  algebraic equations,

$$-2\omega_j \alpha_j [\beta_0 + j(\beta_1 - \beta_0)] = \sum_{kmn} S_{kmn}^{(j)} \alpha_k \alpha_m \alpha_n, \quad (19)$$

for  $j_{\max} + 3$  unknowns  $(\beta_0, \beta_1, \{\alpha_j\})$ . The equations for  $j = 0, 1$  may be used to eliminate  $(\beta_0, \beta_1)$ , leaving  $j_{\max} - 1$  equations to be solved for  $\{\alpha_j\}$  and two parameters of underdetermination. The scaling symmetry allows for elimination of one parameter, so we set  $\alpha_{j_r} = 1$  for some fixed  $0 \leq j_r < j_{\max}$ . Taking the remaining free parameter to be  $\alpha_{j_r+1}$  and requiring solutions to be insensitive to the value of  $j_{\max}$  (i.e., stable to truncation), it is straightforward to construct solutions perturbatively in  $\alpha_{j_r+1}/\alpha_{j_r}$ . We find a single solution for  $j_r = 0$  and precisely two otherwise (see Fig. 1).

*Stability of quasiperiodic solutions.*—Reference [6] extended single-mode, time-periodic solutions to higher order in  $\epsilon$  and found these solutions to be stable to perturbations. Similarly, we examine the stability of our extended class of quasiperiodic solutions, both using full numerical relativity simulations and by numerically solving the TTF ordinary differential equations.

We consider initial data  $A_j(0) = \epsilon \exp(-\mu j)/(2j + 3)$ , which well approximate  $j_r = 0$  quasiperiodic solutions. Varying  $\mu$  and also adding random perturbations, we observe periodic oscillations about the quasiperiodic solution, providing evidence for stability (see Fig. 2). For smaller values of  $\mu$ , energy levels are more closely spaced, resulting in more rapid energy transfers between modes, leading to larger-amplitude oscillations. Likewise, larger random perturbations increase the amplitude of oscillation,

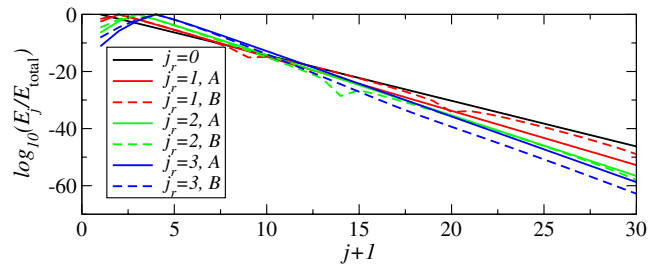


FIG. 1 (color online). Energy spectra of quasiperiodic solutions with  $\alpha_{j_r+1}/\alpha_{j_r} = 0.1$  for  $j_r = 0, 1, 2, 3$ . Dashed and solid lines distinguish different branches for  $j_r > 0$ . The solid branch is well approximated by an exponential to each side of  $j_r$ . For  $\alpha_{j_r+1}/\alpha_{j_r}$  too large, it becomes difficult to obtain solutions to Eq. (19), but for  $j_r = 0$ , we can go up to  $\alpha_1/\alpha_0 \approx 0.42$ . (Constructed for  $j_{\max} = 30$ .)

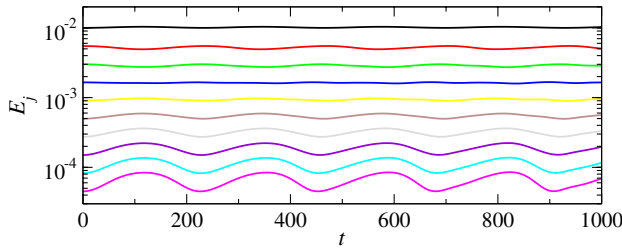


FIG. 2 (color online). Energy per mode for  $0 \leq j \leq 9$  for TTF solution with initial data  $A_j(0) \propto \exp(-0.3j)/(2j+3)$ .

as the initial data deviate more strongly from a quasiperiodic solution. Results from TTF and full numerical relativity simulations are in close agreement.

*Two-mode initial data.*—Our main interest is to understand which initial conditions can be expected to collapse. Thus, it is necessary to study initial data that are *not* expected to closely approximate a quasiperiodic solution. A particularly interesting case consists of two modes initially excited (all others zero), as this case was key to the argument of Ref. [5] showing the onset of the turbulent cascade. In contrast to the results of the previous section, two-mode initial data

$$A_j(0) = \frac{\epsilon}{3}(\delta_j^0 + \kappa\delta_j^1) \quad (20)$$

involves considerable energy transfer among modes provided  $\kappa$  is sufficiently large. [For  $\kappa \ll 1$ , Eq. (20) may be considered as a perturbation about single-mode data.] We examined several choices of  $\kappa$  using both TTF and full numerical relativity, with similar results. Here, we restrict to  $\kappa = 3/5$ , the equal-energy case.

The upper envelope of  $\Pi^2(x=0)$  is often used as an indicator of the onset of instability [5,7,11]. We plot this quantity in Fig. 3, for both full GR simulations and TTF solutions with varying  $j_{\max}$ . In the full GR simulation,  $\Pi^2(x=0)$  grows initially, but in contrast to the blowup observed in Ref. [5] for Gaussian scalar field profile, it then decreases close to its initial value. This *recurrence* phenomenon repeats and—for sufficiently small  $\epsilon$ —collapse never occurs for as long as we have run the simulation. Recurrence was also observed in previous work [11] for broadly distributed Gaussian profiles.

Also in Fig. 3, TTF solutions appear to converge to the full numerical GR solution as  $j_{\max}$  is increased. (Strictly speaking, the TTF and numerical approaches converge as both  $j_{\max} \rightarrow \infty$  and  $\epsilon \rightarrow 0$ ; see the accompanying Supplemental Material for more discussion [15].) This nicely illustrates the cascade-collapse mechanism: Higher- $j$  modes are more sharply peaked at  $x=0$ , so as the (conserved) energy is transferred to these modes,  $\Pi^2(x=0)$  attains higher values. Truncating the system at finite  $j_{\max}$  artificially places a bound on values of  $\Pi^2(x=0)$  that can be reached. In particular,  $\Pi^2(x=0)$  can never blow up for  $j_{\max} < \infty$ .

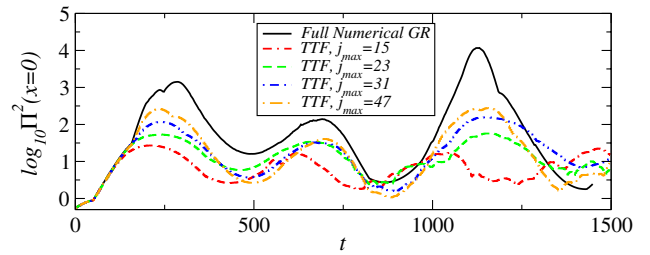


FIG. 3 (color online). Full numerical and TTF results for two-mode equal-energy initial data with  $\epsilon = 0.09$ . As  $j_{\max}$  is increased, the TTF solutions achieve better agreement with the full numerics. Recurrence behavior observed in the full numerical solution is reasonably well captured by the TTF.

It is useful to examine the solution mode by mode, and in Fig. 4 we show the energy per mode as a function of time. Initially, energy is distributed evenly between modes  $j=0,1$ . It then flows out of mode  $j=1$  to mode  $j=2$ , then  $j=3$ , etc. At some point in time, energy begins to flow *back* to mode  $j=1$ , an “inverse energy cascade.” By  $t \approx 450$ , the state has nearly returned to the original configuration. This recurrence behavior then repeats.

The bottom plot of Fig. 4 illustrates the running time-average energy per mode  $\bar{E}_j(t) \equiv t^{-1} \int_0^t E_j(t') dt'$ . Rather than cascading to ever-higher modes, the energy sloshes primarily between low- $j$  modes, in a “metastable” state. We

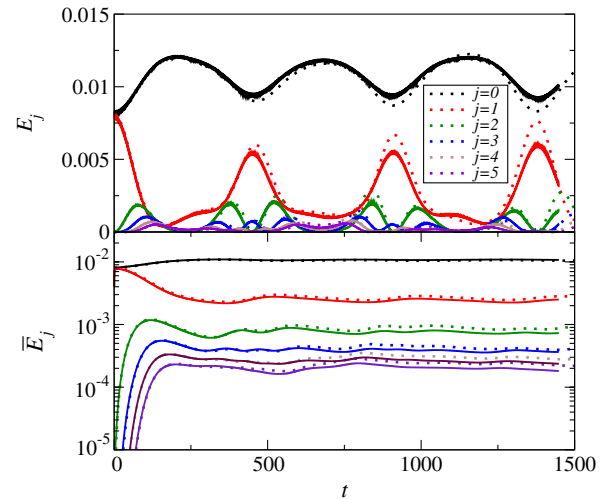


FIG. 4 (color online). Full numerical (solid lines) and TTF (dotted lines) energy (top panel) and running time-average energy (bottom panel) per mode, for two-mode equal-energy initial data. Notice the repeated approximate return of the initial energies to the first two modes in the top panel. In the bottom panel, the running time-average energies approach distinct asymptotic values. For this run with  $j_{\max} = 47$ ,  $\sum_{j=0}^{11} |E_j^{\text{TTF}} - E_j^{\text{numerical}}|/E^{\text{total}}$  does not exceed 0.19. For  $j_{\max} = (31, 23, 15)$ , the bounds are (0.28, 0.42, 0.57). (The horizontal offset is partially attributed to a slight difference in time normalization for our numerical and TTF codes.)

never observe thermalization; i.e., no equipartition of energy occurs.

Figure 4 is remarkably similar in appearance to plots of FPUT [12] (cf. Figs. 4.1 and 4.2 of Ref. [16].) FPUT numerically simulated a collection of nonlinearly coupled harmonic oscillators and expected to see thermalization. Instead, they observed the same recurrence we see here. Indeed, as the TTF formulation (17) of our system makes clear, small-amplitude scalar collapse in AdS reduces precisely to a (infinite) set of nonlinearly coupled oscillators, so the similar behavior should not be surprising. More precisely, our system is related to the FPUT- $\beta$  model [16]. (Of course, the particular resonances and nonlinear interactions differ between our system and FPUT.) Predicting when the FPUT system of oscillators thermalizes is a longstanding problem in nonlinear dynamics and is, indeed, known as the FPUT *paradox* [16–18].

*Discussion.*—Common intuition suggests that a finite-sized strongly interacting system driven off equilibrium, even by a small amount, eventually thermalizes. This thermalization would imply, via AdS/CFT, that arbitrarily small perturbations about global AdS *must* result in gravitational collapse. However, we have uncovered in this Letter a large class of initial conditions for a massless, self-gravitating real scalar field in AdS<sub>4</sub> that appears to *avoid* collapse. We constructed and evolved these initial conditions within a newly proposed TTF as well as through full numerical GR simulations. TTF shows that scalar perturbations of AdS are in the same universality class as the famous FPUT problem [12]. Thus, perturbed AdS spacetimes act as a holographic bridge between nonequilibrium dynamics of CFTs and the dynamics of nonlinearly coupled oscillators and the FPUT paradox. In this Letter we focused on the dynamics of low-energy (2 + 1)-dimensional CFT excitations “prepared” with nonzero expectation values of dimension three (marginal) operators. Extensions to higher-dimensional CFTs as well as to states generated by (ir)relevant operators are straightforward.

We would like to thank A. Polkovnikov and J. Santos for interesting discussions and correspondence. We also thank D. Minic and A. Zimmerman for pointing us to the FPUT problem. Finally, we thank P. Bizoń and A. Rostworowski for discussions and direct comparison of numerical solutions. This work was supported by the NSF under Grants No. PHY-0969827 and No. PHY-1308621 (LIU), NASA under Grant No. NNX13AH01G, NSERC through a Discovery Grant (to A. B. and L. L.) and CIFAR (to L. L.). S. R. G. acknowledges support by a CITA National Fellowship. L. L. and S. L. L. also acknowledge the Centre for Theoretical Cosmology at the University of Cambridge for their hospitality and its participants for helpful discussions at the “New Frontiers in Dynamical

Gravity” meeting during which this work was completed. Research at Perimeter Institute is supported through Industry Canada and by the Province of Ontario through the Ministry of Research & Innovation. Computations were performed at Sharcnet.

\*vbalasu8@uwo.ca

†abuchel@perimeterinstitute.ca

‡sgreen04@uoguelph.ca

§llehner@perimeterinstitute.ca

||steve.liebling@liu.edu

- [1] O. Aharony, S. S. Gubser, J. M. Maldacena, H. Ooguri, and Y. Oz, *Phys. Rep.* **323**, 183 (2000).
- [2] P. M. Chesler and L. G. Yaffe, *Phys. Rev. Lett.* **102**, 211601 (2009).
- [3] V. Balasubramanian, A. Bernamonti, J. de Boer, N. Copland, B. Craps, E. Keski-Vakkuri, B. Müller, A. Schäfer, M. Shigemori, and W. Staessens, *Phys. Rev. Lett.* **106**, 191601 (2011).
- [4] A. Buchel, R. C. Myers, and A. van Niekerk, *Phys. Rev. Lett.* **111**, 201602 (2013).
- [5] P. Bizoń and A. Rostworowski, *Phys. Rev. Lett.* **107**, 031102 (2011).
- [6] M. Maliborski and A. Rostworowski, *Phys. Rev. Lett.* **111**, 051102 (2013).
- [7] A. Buchel, L. Lehner, and S. L. Liebling, *Phys. Rev. D* **86**, 123011 (2012).
- [8] M. Maliborski and A. Rostworowski, *Phys. Rev. D* **89**, 124006 (2014).
- [9] O. J. Dias, G. T. Horowitz, D. Marolf, and J. E. Santos, *Classical Quantum Gravity* **29**, 235019 (2012).
- [10] J. Abajo-Arastia, E. da Silva, E. Lopez, J. Mas, and A. Serantes, *J. High Energy Phys.* **05** (2014) 126.
- [11] A. Buchel, S. L. Liebling, and L. Lehner, *Phys. Rev. D* **87**, 123006 (2013).
- [12] E. Fermi, J. Pasta, and S. M. Ulam, Technical Report No. LA-1940, 1955; also in *Enrico Fermi: Collected Papers*, edited by (University of Chicago Press, Chicago, 1965), Vol. 2.
- [13] T. Dauxois, *Phys. Today*, **61**, 1, 55 (2008).
- [14] J. Kevorkian and J. D. Cole, *Multiple Scale and Singular Perturbation Methods*, Applied Mathematical Sciences, Vol. 114 (Springer, New York, 1996).
- [15] See the Supplemental Material at <http://link.aps.org/supplemental/10.1103/PhysRevLett.113.071601> for additional description of approximations involved in TTF, expectations for convergence in both  $\epsilon$  and  $j_{\max}$ , and results of tests validating our full GR code.
- [16] G. Benettin, A. Carati, L. Galgani, and A. Giorgilli, *The Fermi-Pasta-Ulam Problem and the Metastability Perspective*, Lecture Notes in Physics, Vol. 728 (Springer, Berlin, 2008).
- [17] P. Poggi, S. Ruffo, and H. Kantz, *Phys. Rev. E* **52**, 307 (1995).
- [18] G. P. Berman and F. M. Izrailev, *Chaos* **15**, 015104 (2005).